
PERGAMON

Journal of Quantitative Spectroscopy & Radiative Transfer 81 (2003) 19–30

Journal of Quantitative Spectroscopy & Radiative Transfer

www.elsevier.com/locate/jqsrt

X-ray spectroscopy of a thin foil plasma produced by a short-pulse high-intensity laser

P. Audebert[a,*], V. Nagels[a], J.P. Geindre[a], F. Dorchies[b], O. Peyrusse[c], S. Gary[c], F. Girard[c], R. Shepherd[d], J.C. Gauthier[a], C. Chenais-Popovics[a]

[a] *LULI, UMR No 7605 CNRS, CEA, Ecole Polytechnique, Univ. Paris VI, Palaiseau 91128, France*
[b] *CELIA, Université Bordeaux 33405 Talence, France*
[c] *Commissariat à l'Energie Atomique, Bruyères-le-Châtel 91680, France*
[d] *Lawrence Livermore National Laboratory, P.O. Box 808, Livermore, CA 94550, USA*

Accepted 15 February 2003

Abstract

High density and temperature plasmas have been generated by irradiating thin foils of various elements with a high-energy subpicosecond laser pulse. The X-ray emission duration was studied by time-resolved X-ray spectroscopy. Frequency domain interferometry provided a measurement of the hydrodynamic expansion of the back of the foil as a function of time. The effect of longitudinal temperature gradients, i.e., gradients perpendicular to the surface, were decreased using very thin foil targets. Additionally, radial gradients effects, i.e., gradients parallel to the surface, were limited by using a 50 μm pinhole on target. The Al, Se and Sm spectra, recorded in the range 7.7–8 Å using a conical crystal spectrometer coupled to an 800 fs resolution streak camera, lasted a few picoseconds. Sm spectra showed no spectral features in this wavelength range, providing a spectrally homogeneous backlighter for future experiments. The main features of the experimental time-resolved spectra have been well reproduced with one-dimensional hydrodynamic simulations of the free expansion of a plasma heated at a given initial temperature obtained from the expansion velocity of the rear critical surface of the plasma.

Keywords: High density plasma; Short pulse laser; X-ray spectroscopy

1. Introduction

Many groups have recorded X-ray spectra emitted from solid targets heated with an ultra-short laser pulse [1–8]. Typically, these experiments have been performed with the laser light focused

* Corresponding author.
E-mail address: patrick.audebert@polytechnique.fr (P. Audebert).

0022-4073/03/$ - see front matter © 2003 Elsevier Science Ltd. All rights reserved.
doi:10.1016/S0022-4073(03)00049-9

on a thick solid target. With a high contrast pulse, inverse Bremsstrahlung heats the several skin depths—tens of nanometers—interaction region, while high-energy, suprathermal electrons, produced by resonance absorption, heat the solid matter deep inside the target. The suprathermal electrons deposit their energy far from the laser focal spot [9,10], so that large longitudinal spatial gradients are produced. As a result, interpretation of X-ray emission from this type of plasma is very difficult to perform. Although some of these previous experiments have used fast X-ray streak cameras to time resolve ($\sim$1 ps) the X-ray emission [11,12], most experiments have been performed with time-integrated X-ray diagnostics.

To minimize the problems associated with longitudinal temperature gradients, sub-100 nm aluminum foil targets have been used in a number of X-ray emission experiments. With a foil thickness much smaller than the thermal penetration depth [13], the entire target should be heated uniformly at constant density because electron conduction propagates the laser heating over the foil thickness before significant hydrodynamic motion occurs. Previous experimental studies [4,12] have compared the time scale in the evolution of K-shell X-ray emission to the cooling rate controlled by hydrodynamic plasma expansion. Later studies on thin foils with a sub-picosecond time resolution were focused on the time history of the He-like $1s^2$-1s2p emission [14] and the effect of the laser pulse duration. Time-resolved measurements of He-like lines from thin foils [15] and from buried layers [16] have been published recently and addressed questions concerning the large emission of the He-like satellites obtained in these conditions.

In contrast, the effect of radial gradients on the duration of X-ray emission has never been investigated. In particular, the cooler plasma located in the outer regions of the focal spot could modify the X-ray duration and its spectral profile. In this paper, we refine previous studies of the sub-picosecond dynamics of the K-shell emission from thin aluminum foils heated with a high-intensity, high-contrast, ultrashort pulse laser. In particular, we investigate the question of the radial gradients by limiting the lateral extent of the observed X-ray emission with a pinhole included in the target design. Additionally, we improve the study by using frequency domain interferometry (FDI) which provided a measurement of the hydrodynamic expansion of the plasma independently of the time-resolved spectra. Our study was also extended to higher-Z material using thin selenium and samarium foils.

2. Experimental setup: targets and diagnostics

2.1. Laser and target conditions

We have performed experiments on thin foils of low, intermediate, and high-Z elements at the LULI 100 Terawatt laser facility to study the time dependence of the X-ray emission of laser-heated solids. To suppress the ASE effect, the laser was frequency doubled ($\lambda = 0.53$ μm), and S-polarized light was used to minimize resonance absorption. The laser energy was varied by a factor of 10, and the focal spot diameter was also changed by a factor of 2 to cover a range of intensities from 2×10^{17} to 8×10^{18} W/cm^2. The atomic number of the target elements was chosen to cover low- and high-Z: aluminum ($Z = 13$), selenium ($Z = 34$) and samarium ($Z = 62$). To decrease the effect of longitudinal temperature gradients, very thin foil targets were used (80 nm of Al, 44 nm of Se and 33 nm of Sm, equivalent to about 20 μg/cm^2 for the three elements). We have particularly studied the effect of radial gradients by limiting the observed X-ray emission region using a target with a

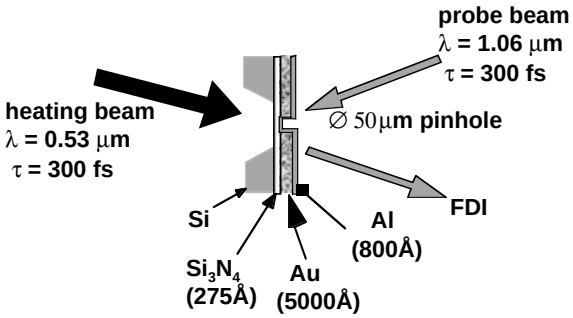

Fig. 1. Configuration of the pinhole targets used to limit lateral gradients. For better understanding scales are not respected.

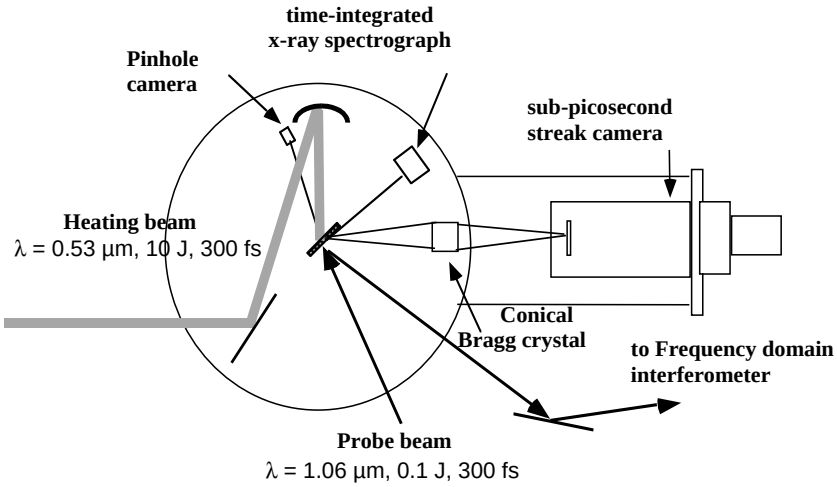

Fig. 2. Experimental setup.

gold pinhole incorporated. The geometry of the targets that included the pinhole is shown in Fig. 1. The target is constructed by depositing a 25 nm silicon nitride layer on a silicon wafer. Next a 300 μm hole was made in the silicon wafer, leaving a silicon nitride membrane. This membrane supported an Au pinhole, which was either a 50 or 100 μm diameter hole lithographically produced from a 0.5 μm Au deposition. Finally, an Al, Se, or Sm layer was deposited on the rear surface, see Fig. 1.

2.2. Time-resolved spectroscopy

Time-resolved spectra were recorded in the range 7.7–8 Å, using a conical thallium-hydrogen-phthalate (TlAP) crystal spectrometer [17,18] coupled to an 800 fs resolution streak camera [19]. This geometry is necessary to focus X-rays in the plane of the photocathode, the camera being mounted on a flange of the experimental chamber as shown in Fig. 2. The crystal setting can be modified to change the focusing of the crystal: the width of the focal line can be easily varied from

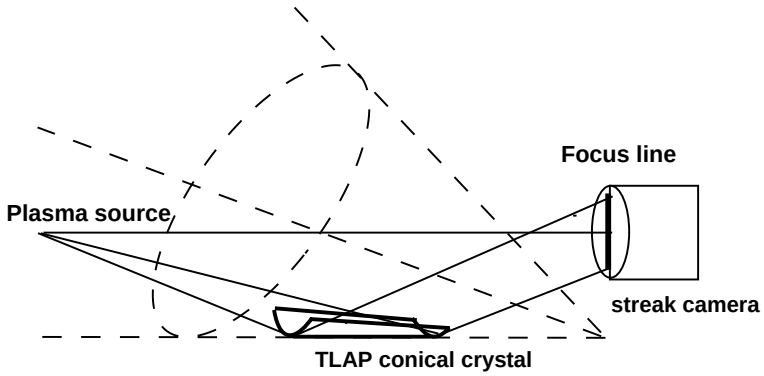

Fig. 3. Mounting of the conical TlAP crystal coupled with an X-ray streak camera.

10 to 100 μm without changing the wavelength range, which permits one to change the intensity on the streak camera slit. In Fig. 3 we show the details of the mounting of the Bragg crystal with respect to the streak camera slit.

The 7.7–8.4 Å spectral region is of interest to diagnose K-shell emission from aluminum plasmas. Indeed, this region covers the Al^{11+} resonance line $1s^2$–1s2p and its satellites. It is also the region where the Kα inner shell $n = 1$–2 transitions belonging to Al^{4+} to Al^{11+} can be observed. Because samarium can be used as a backlighter to measure the 1s–2p transitions of aluminum by absorption spectroscopy in low temperature plasmas, we have measured its spectrum in the same spectral region. The range covered by the crystal was larger than the slit length, and we chose to set the slit on the Al Heα line, i.e., from 7.7 to 8 Å.

The X-ray pulse duration has been measured with an uncertainty of less than 0.5 ps. The dynamic range of the streak camera is rather poor: a factor of 100 saturates the electronics of the camera. We have measured this saturation by using a filter wheel mounted with 2, 3, or 4 layers of 10 μm thick mylar, permitting the variation of the signal intensity by a factor of 100. Fig. 4 shows a samarium spectrum filtered with 2, 3 and 4 layers of mylar. One can see in Fig. 4b that saturation effects increase the measured pulse duration by a factor of 2. When the spectrum is flat as in the case of samarium, there is no indication of this saturation, except the signal level measured on the CCD camera coupled to the streak camera. In our case, using an intensifier between the phosphor of the streak camera and the CCD, the signal had to be less than 75 counts over the background of the CCD. In the case, where spectral line transitions occur, as in the aluminum spectrum, saturation can be detected by the fact that saturated lines start earlier than the unsaturated parts of the spectrum.

2.3. Frequency-domain interferometry

An FDI of the rear of the foil was used to provide a measurement of the hydrodynamic expansion as function of time for each shot. We used a Mach–Zehnder interferometer in which amplitude division is used to obtain spectral information in a single shot. The principles of FDI have been described previously [20]. Fig. 5 gives a schematic view of the experimental mounting. A probe beam (100 mJ in a 15 ps duration chirped pulse) was reflected from the target. The plasma was imaged on the entrance beam-splitter prism of the Mach–Zehnder interferometer that was set with slightly

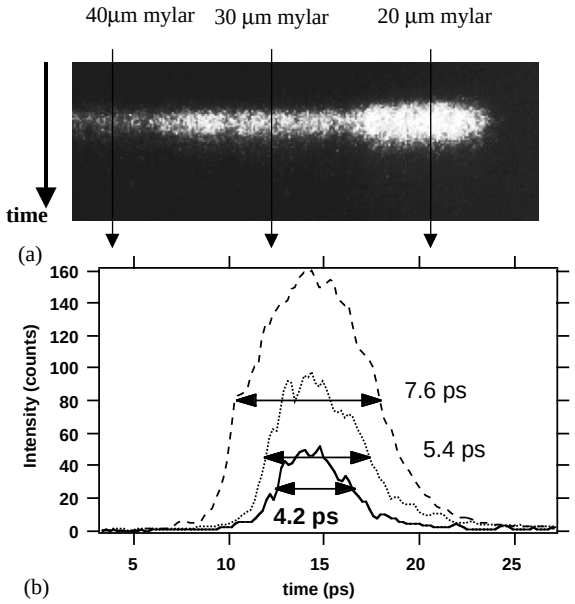

Fig. 4. Time-resolved spectrum of samarium. (a) Raw image. The three regions of the image are filtered by 20, 30 and 40 μm thick mylar foil. The trace positions are indicated. (b): traces in saturated and unsaturated regions of the image.

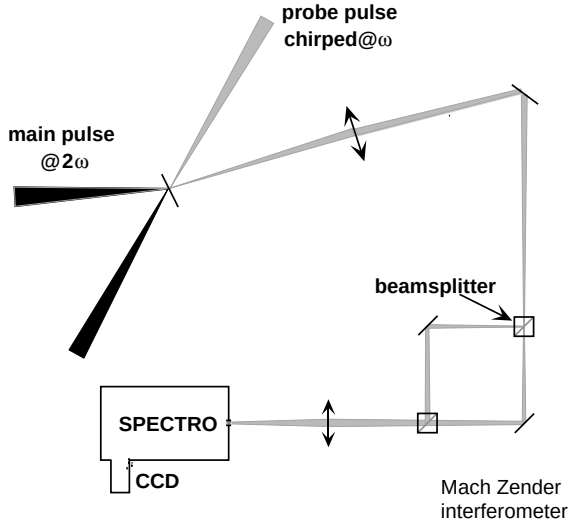

Fig. 5. Schematic of the mounting of the FDI diagnostic.

unequal arms. The entrance prism was imaged again on the entrance slit of a 1-m Czerny–Turner spectrometer and a 12-bit CCD camera recorded the spectrum. A calibration shot, without the main laser beams, was necessary to define the instrumental null phase. More details on the experimental system and of the signal analysis are given elsewhere [21,22]. To summarize, the complex reflection

coefficient $R(\omega)$ and the phase shift $\Delta\Phi(\omega)$ are extracted from the comparison of the signal and reference shots, with the method described in Ref. [23]. With the knowledge of the probe pulse chirp parameter a, which is determined experimentally, the perturbation in time can be recovered. Indeed, the field of the chirped pulse E_{oc} can be written in the frequency domain,

$$E_{oc}(\omega) = \mathscr{F}[E_{oc}(t)] = E_0(\omega)\exp\{j(\omega - \omega_0)^2/a\}$$

with E_0 the field of the laser pulse, ω_0 the central frequency and a the coefficient of the linear frequency chirp.

We construct the signal by multiplying the field by the plasma perturbation, so that,

$$E(\omega) = E_{oc}(\omega)\sqrt{R(\omega)}\exp[j\Delta\phi(\omega)].$$

With $R(\omega)$ the plasma reflectivity and $\Delta\phi(\omega)$ the thase variation due to the plasma. The perturbation due to the plasma $P(t)$ in the time domain can be now easily recovered by using an inverse-Fourier transform

$$P(t) = \mathscr{F}^{-1}[E(\omega)]/E_{oc}(t),$$

where $E_{oc}(t)$ is the original chirped pulse in the time domain. With this signal reconstruction procedure, based on the knowledge of the chirp parameters, we reach a time resolution comparable to the compressed probe pulse duration, i.e., about 500 fs. We stress that the present measurements are taken in a single shot.

3. Time-resolved X-ray spectra

Al, Se and Sm spectra have been recorded as a function of time, for laser intensities of 1 and 10 J, for different focusing conditions, and for different types of targets. All the thin foil data are measured at the rear of the foil, with or without a pinhole.

3.1. Aluminum spectra

For the Al experiments the laser intensity was 2×10^{18} W/cm^2, the 10 J laser energy being focused in a 20 μm diameter focal spot. Spectra measured on thin foils (with and without a 50 μm diameter pinhole) are shown in Fig. 6. The resonance He-like line $1s^2$–$1s2p$ (Heα) and its dielectronic Li-like satellites are indicated, and are surrounded by a low-level continuum. The duration of the Heα resonance line emission is always longer than the satellites. Fig. 7 shows the time axis traces obtained from Fig. 6 for the Heα line, the satellites, and the continuum. With the pinhole target all emission has a shorter duration: the Heα emission lasts 6 ps full-width-half-maximum (FWHM); the satellite emission lasts ~ 3 ps; and the continuum is shorter, between 1 and 2 ps. The fact that the emission is of a shorter duration when observed through a pinhole shows that lateral gradients play a role in the interaction. On the other hand, it is found that the duration of the emission was longer for a massive target. For example, the Heα emission duration was 7.7 ps FWHM, but there is an extended recombination phase that followed this rather short peak emission phase.

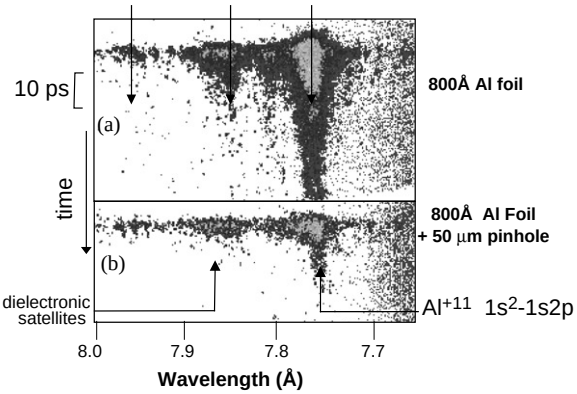

Fig. 6. Time-resolved X-ray images obtained for different aluminum targets: (a) 800 Å Al thin foil; (b) 800 Å Al thin foil observed through a 50 μm diameter pinhole. The positions of the traces presented in Fig. 7 are indicated, and correspond to the Heα line, to the satellites and to the continuum.

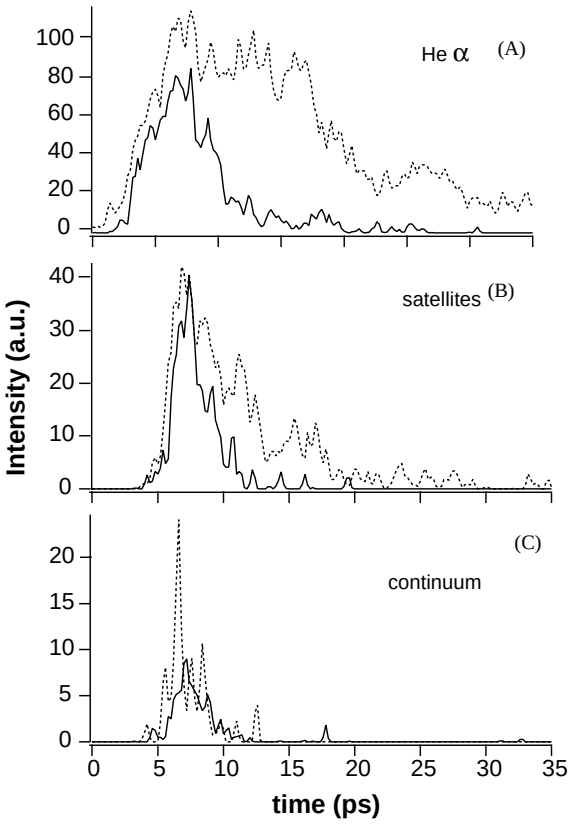

Fig. 7. X-ray emissions as a function of time corresponding to the two types of targets shown in Fig. 6. Dotted line: 800 Å Al thin foil. Solid black line: 800 Å Al thin foil observed through a 50 μm diameter pinhole. (A): Heα line; (B) satellites; (C) continuum.

3.2. Spectra of heavier elements

The duration of samarium emission has also been measured for different targets and laser conditions. First it has to be noted that the samarium spectra are completely featureless in the measured spectral range. This is completely different from spectra obtained with nanosecond laser pulses, as many lines corresponding to 3d–4f transitions are present in this spectral region. This means that samarium, and probably other heavy elements, may provide spectrally smooth backlighters for absorption spectroscopy. The measured pulse duration of samarium was in the range of a few picoseconds. With low laser energy (1 J yielding $\sim 2\times 10^{17}$ W/cm^2) a FWHM pulse duration of about 2 ps was measured; however, for higher laser intensity this value could rise to 4 ps FWHM. This value was decreased to 2.5 ps by measuring X-rays at high laser intensity through a 100 μm pinhole, in agreement with the trend found for the Al pinhole restricted observations.

The selenium spectrum exhibited 2p–3d lines in the measured spectral range. In particular, the Ne-like transitions of $Se^{24+}2p^6\,^1S_0$–$2p^5 3d\,^3D_1$ at 7.70 Å and $2p^6\,^1S_0$–$2p^5 3d\,^1P_1$ at 7.88 Å were measured. The $^3D_1$ transition always had a slightly longer emission duration than the $^1P_1$ line. This difference is unexplained until now. These transition lasted 6–8 ps FWHM for high laser intensity (8×10^{18} W/cm^2) and 3.5–4.5 ps for a lower laser intensity (2×10^{18} W/cm^2). The continuum was slightly shorter (1 or 2 ps less), as in the case of aluminum.

4. Frequency domain interferometry data analysis

FDI provided, as a function of time and space, the phase of the probe pulse reflected at the back of the thin foil. In Fig. 8 we show the measurement obtained for an 80 nm thick Al foil constrained by a 50 μm pinhole irradiated with an intensity of 8×10^{18} W/cm^2. The 2D plot shown in Fig. 8a shows that the phase changed only over the 50 μm diameter of the pinhole. Also, the phase change was homogeneous along the pinhole, suggesting that the X-ray spectra recorded from this shot were emitted by a 1D expanding plasma. In Fig. 8b we plot the trace from the center of the 50 μm pinhole. It shows that, after a few picoseconds the phase rise linearly, indicating a constant expansion velocity.

The phase of the probe beam reflected on the back of the foil is linked to the motion of the critical density of the expanding plasma. In the case of a self-similar expansion, the position of the density at the turning point of the probe pulse would be proportional to the sound speed of the plasma. In our experiment, the motion is not a pure self-similar expansion, so a simple 1D hydrodynamic isothermal expansion Lagrangian code was used [24]. The isothermal hypothesis was justified by hydrodynamic simulations run with the code FILM demonstrating that the temperature is spatially uniform in the expanding plasma.

In our model, we assume a uniform initial density equal to the solid density, an adjustable initial peak temperature T_0, and a stationary ionization given by the TKN model [25]. The phase change of the probe pulse as function of time is then calculated with only one unknown parameter, the initial temperature T_0 of the foil, the density and foil thickness being fixed. In Fig. 8b the best fit of the phase is shown, which is obtained for an initial temperature of $T_0 = 1.2$ KeV. This value is the uniform temperature achieved at the peak of the heating pulse in the plasma.

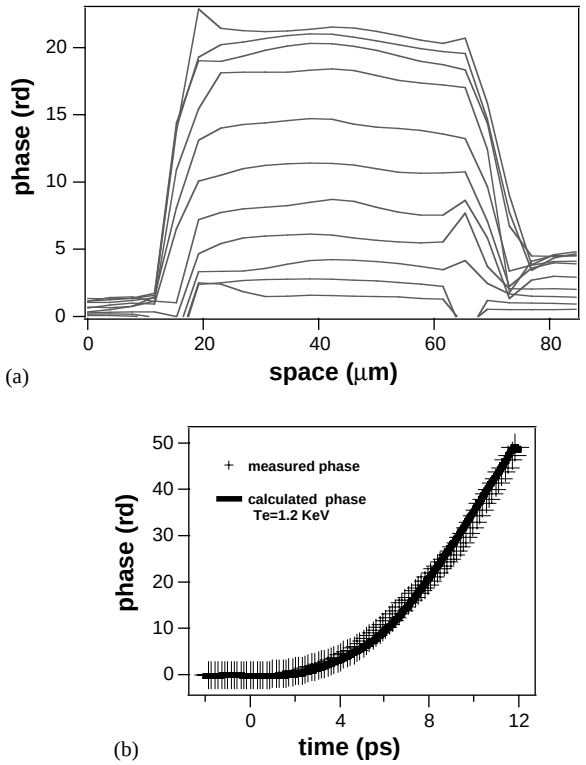

Fig. 8. FDI results. (a) Plot of the phase: each curve represents the phase as a function of space for a given time; curves are separated by 500 fs. (b) The phase as a function of time, along the trace, at the center of the pinhole. Time zero is arbitrarily chosen.

5. Data analysis

To obtain detailed information on laser plasma emission, an investigation using hydrodynamic simulations post-processed by a collisional-radiative model is usually performed. This type of analysis is not possible for the present short-pulse high-intensity experimental conditions, because the fluid description of hydrodynamics codes fails for this very high intensity case where the ponderomotive pressure of the laser light is much higher than the thermal pressure [22]. However, quite uniform temperature and density conditions in the direction perpendicular to the target surface are expected here, even for times larger than 500 fs after the laser peak. Then, the expansion of the foil could be described with the 1D hydrocode FILM, as the free expansion of a foil heated uniformly at a given temperature. This initial foil temperature is probably reached in less than 100 fs after the laser pulse maximum. In the present experiment it was fixed at 1.2 keV the value obtained by the FDI measurement, see Section 4. Further justification for this approach is found in the fact that, due to the finite experimental time resolution, the observed spectra are recorded mainly during the recombination phase of the plasma.

The time-resolved spectra were calculated by post-processing FILM with the collisional-radiative code AVERROES/TRANSPEC [26]. In the present calculations of the time-dependent populations

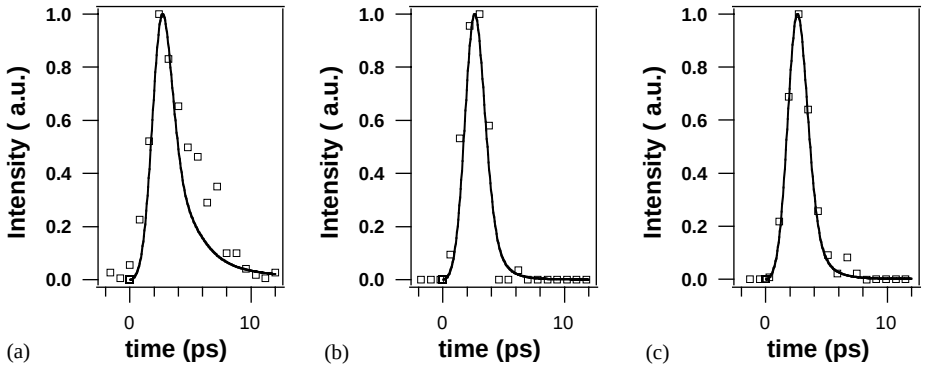

Fig. 9. Emission of the aluminum emission as a function of time, as measured for a 80 nm foil observed through a 50 μm pinhole (squares), and as simulated by the code FILM (solid line) post-processed by the atomic code AVERROES/TRANSPEC. (a) Heα line, at 7.75 Å; (b) satellite lines at 7.84 Å; (c) continuum at 7.89 Å.

of Al, only line transfer of the resonance line, Heα, has been taken into account. As satellite lines contribute largely to the emission, the great number of levels required to calculate the spectrum were modeled by superconfiguration accounting as described in Ref. [15]. This was performed for all the ions from Al I to Al XI where superconfigurations with quantum numbers up to $n = 5$ and superconfigurations with a vacancy in the 1s shell were taken into account.

In Fig. 9 we plot the experimental and simulated time histories of the Heα ($1s^2$–$1s\,2p\ ^1P$) line at 7.75 Å, of the satellites at 7.87 Å and of the continuum emission at 7.89 Å, obtained for a heated 80 nm thin foil, and measured through a 50 μm pinhole. The data are convolved with a 1 ps FWHM Gaussian to take into account the finite time resolution of the spectrometer coupled to the streak camera. The main features of the time-resolved spectra are reproduced quite accurately for the three different spectral features modeled. It has to be noted that the fit is good because the observed plasma is monodimensional. This is due to the small radial extent of the observed plasma, limited by a 50 μm pinhole.

6. Conclusion

The sub-picosecond dynamics of the K-shell X-ray emission from thin foils heated with a high-intensity, high-contrast, ultra-short pulse laser were studied by comparison with hydrodynamic and atomic simulations. A better understanding is made possible by the pinhole imaging of the emission which restricts the observed spectral data to the laser irradiated spot and eliminates the surrounding plasma that is created by other mechanisms.

X-ray pulse durations measured for Al, Se and Sm thick and thin foils were measured to be in the 1–10 ps range. Limiting the radial extent of the observed plasma by a pinhole has proved to be essential for the understanding of the X-ray emission spectra. The presence of a cooler plasma located around the focal spot, which emits for a longer time, unduly complicates the data analysis.

FDI demonstrated the uniformity of the plasma in the radial dimension over the pinhole diameter and provided a measurement of the electron temperature (1.2 keV) at the laser pulse peak.

Hydrodynamics of the experiment was modeled by a free expanding plasma heated instantly to the 1.2 keV temperature measured by the FDI diagnostic. Using this hydrodynamic expansion model, the X-ray duration of the spectrum measured through a 50 μm pinhole was calculated by the AVERROES/TRANSPEC atomic code, in very good agreement with the experiment.

Future work will be done to simulate Se and Sm in similar conditions with a radiative hydrodynamic code. For aluminum, the code AVERROES/TRANSPEC will be improved by introducing a better model of the spectral line profiles, in particular Stark broadening which can play a role for the very large density achieved in the plasmas produced by high-energy, ultra-short laser pulses.

Acknowledgements

The authors want to thank the staff of the LULI facility for technical assistance, and the target preparation laboratory in Livermore Lawrence National Laboratory.

References

[1] Audebert P, Geindre J-P, Rousse A, Falliès F, Gauthier J-C, Mysyrowicz A, Grillon G, Antonetti A. K-shell emission dynamics of Be-like to He-like ions from a 100 fs laser-produced aluminium plasma. J Phys B 1994;27:3303–14.

[2] Gauthier J-C, Geindre J-P, Audebert P, Bastiani S, Quoix C, Grillon G, Mysyrowicz A, Antonetti A, Mancini RC. Theoretical and experimental studies of laser-produced plasmas driven by high-intensity femtosecond laser pulses. Phys Plasmas 1997;4:1811–20.

[3] Altenbernd D, Teubner U, Gibbon P, Förster E, Audebert P, Geindre J-P, Gauthier J-C, Grillon G, Antonetti A. Soft X-ray brilliance of femtosecond and picosecond laser-plasmas. J Phys B 1997;30:3969–82.

[4] Kieffer J-C, Jiang Z, Ikhlef A, Côté CY, Peyrusse O. Picosecond dynamics of a hot solid-density plasma. J Opt Soc Am B 1996;13:132–7.

[5] Côté C, Kieffer J-C, Jiang Z, Ikhlef A, Pépin H. KeV X-ray emission produced by a sub-picosecond laser interacting with a controlled preformed plasma. J Phys B 1998;31:L883–9.

[6] Saemann A, Eidmann K, Golovkin IE, Mancini R, Anderson E, Förster E, Witte K. Isochoric heating of solid aluminum by ultrashort laser pulses focused on a tamped target. Phys Rev Lett 1999;82:4843–6.

[7] Eidmann K, Saemann A, Andiel U, Golovkin IE, Mancini RC, Anderson E, Förster E. Generation of hot plasma at solid density by high-contrast ultra-short laser pulses. JQSRT 2000;65:173–84.

[8] Andiel U, Eidmann K, Witte K. Time-resolved X-ray K-shell spectra from high density plasmas generated by ultrashort laser pulses. Phys Rev E 2001;63:26407.

[9] Matte J-P, Kieffer J-C, Ethier S, Chaker M, Peyrusse O. Spectroscopic signature of a non-Maxellian and non-stationary effects in plasmas heated by intense, ultra-short laser pulses. Phys Rev Lett 1994;72:1208–11.

[10] Rosmej FB. Hot electron X-ray diagnostics. J Phys B 1997;30:L819–28.

[11] Côté CY, Kieffer J-C, Peyrusse O. Picosecond time-resolved spectroscopy of a controlled preformed plasma heated by an intense laser pulse. Phys Rev E 1997;56:992–1000.

[12] Shepherd R, More R, Young B, Price D, Walling R, Osterheld A, Stewart R, Kato T. Reduced conduction cooling in high energy-density plasmas using ultra-short pulse laser heated thin foil targets. JQSRT 1997;58:911–6.

[13] Eidmann K, Andiel U, Förster E, Golovkin IE, Mancini RC, Saemann A, Schlegel T, Uschmann I. Spectroscopy of plasmas at solid density generated by ultra-short laser pulses. In: Mancini R, Phaneuf R, editors. Atomic processes in plasmas, AIP Conference Proceedings No. 547, New York: AIP, 2000. p. 238–51.

[14] Gallant P, Jiang Z, Chien C, Forget P, Dorchies F, Kieffer J-C, Pépin H, Peyrusse O, Mourou G, Krol A. Spectroscopy of solid density plasmas generated by irradiation of thin foils with a fs laser. JQSRT 2000;65:243–52.

[15] Audebert P, Shepherd R, Fournier KB, Peyrusse O, Price D, Lee RW, Springer P, Gauthier J-C, Klein L. Time-resolved plasma spectroscopy of thin foils heated by a relativistic-intensity short-pulse laser. Phys Rev E 2002;66:66412.

[16] Andiel U, Eidmann K, Hakel P, Mancini RC, Junkel-Vives GC, Abdallah J, Witte K. Demonstration of aluminum K-shell line shifts in isochorically heated targets driven by ultra-short laser pulses. Europhys Lett 2002;60:861–7.
[17] Marjoribanks RS, Richardson MC, Audebert P, Bradley DK, Gregory GG, Jaanimagi PA. Time-resolved spectroscopy for detailed studies ($\lambda/\Delta\lambda > 1000$) of weak X-ray emitters in laser plasmas. SPIE Proc. (X-rays from Laser Plasmas) 1987;831:185–98.
[18] Hall TA. A focusing X-ray crystal spectrograph. J Phys E Instrum 1984;17:110–2.
[19] Gallant P, Forget P, Dorchies F, Jiang Z, Kieffer J-C, Jaanimagi PA, Rebuffie JC, Goulmy C, Pelletier J-F, Sutton M. Characterization of a subpicosecond X-ray streak camera for ultrashort laser-produced plasmas experiments. Rev Sci Instrum 2000;71:3627–33.
[20] Blanc P, Audebert P, Falliès F, Geindre J-P, Gauthier J-C, Dos Santos A, Mysyrowicz A, Antonetti A. Phase dynamics of reflected probe pulses from sub-100-fs laser-produced plasmas. J Opt Soc Am 1996;13:118–24.
[21] Rebibo S, Geindre J-P, Audebert P, Grillon G, Chambaret J-P, Gauthier J-C. Single shot spectral interferometry of femtosecond laser-produced plasmas. Laser Particles Beams 2001;19:67–74.
[22] Audebert P, Geindre J-P, Rebibo S, Gauthier J-C. Direct observation of the ponderomotive force effects in short-scale-length laser plasmas by frequency-domain interferometry. Phys Rev E 2001;64:56412.
[23] Geindre J-P, Audebert P, Rebibo S, Gauthier J-C. Single-shot spectral interferometry with chirped pulses. Opt Lett 1994;19:1612–4.
[24] Quoix C, Hamoniaux G, Antonetti A, Gauthier J-C, Geindre J-P, Audebert P. Ultrafast plasma studies by phase and amplitude measurements with femtosecond spectral interferometry. JQSRT 2000;65:455–62.
[25] Lee YT, More RM. An electron conductivity model. Phys Fluids 1984;27:1273.
[26] Peyrusse O. A superconfiguration model for broadband spectroscopy of non-LTE plasmas. J Phys B 2000;33: 4303–21.